



# Burnup analysis of rock-like oxide fuel disks irradiated in the Japan Research Reactor No. 3

Y. Nakano <sup>\*</sup>, H. Akie, M. Magara, H. Takano

*Japan Atomic Energy Research Institute, Tokai-mura, Naka-gun, Ibaraki-ken 319-1195 Japan*

## Abstract

Burnup analysis of rock-like oxide (ROX) fuel disks has been carried out and the results have been compared with measured values. Two kinds of ROX disks: zirconia and thoria, were fabricated and irradiated in an irradiation hole of the Japan Research Reactor No. 3 (JRR-3). After irradiation, several post-irradiation examinations (PIE) were performed. Computer codes used for the calculations were the SRAC and the MVP-BURN codes. Firstly, the neutron spectrum in the irradiation hole was calculated using the SRAC code system. Fixed source problems were solved to obtain the neutron spectra and effective cross-sections of the disks and burnup calculations were performed. The calculated results of burnup, isotopic abundance of plutonium and production of americium and curium were compared with measurement values. Calculations overestimate the measured burnup by 7 ~ 15% and both codes largely underestimate the measured production of americium and curium isotopes. The calculated plutonium abundance agrees moderately well with the measured values. © 1999 Elsevier Science B.V. All rights reserved.

## 1. Introduction

Rock-like oxide inert matrix fuel (ROX) [1] is a new fuel concept undergoing feasibility studies for transmuted plutonium, minor actinides and long-life fission products (FP). To perform the study, not only adequate computer programs and methodologies but also neutron cross-section data with high accuracy for transuranium (TRU) nuclides, uranium, thorium and FP nuclides are necessary. One of the best ways to validate codes, methodology and nuclear data accuracy is to analyze good benchmark experimental data. Irradiation tests on ROX samples were carried out in order to obtain material property data for fuel development and benchmark data for burnup analysis.

## 2. ROX disks and irradiation experiment

Two kinds of pieces (15 for each kind) of ROX disks were fabricated at JAERI, one of zirconia type and the

other of thoria type. The composition of the disks is shown in Table 1, and the plutonium isotopic abundance is reported in Table 2. The diameter of a disk is 3 mm and the thickness is 1 mm. Five disks were placed in a pellet case of niobium with 1% zirconium. The pellet case was contained in a fuel case of platinum, which was filled with helium gas at 1 atm. The fuel case was put in a clad tube of niobium–1% zirconium. Two cladding tubes and a fluence monitor were inserted in a sample case of molybdenum. Three sample cases were installed in an instrumented irradiation capsule of aluminum alloy. Fig. 1 shows a horizontal cross-section of the capsule.

The capsules were irradiated during four cycles, representing about 14 weeks, in JRR-3, a swimming pool type research reactor with a maximum thermal output of 20 MW. An irradiation hole in the beryllium reflector was used for the experiment. Temperature in the capsule was controlled to be about 1273 K.

## 3. Post-irradiation examination

After the irradiation, the capsule was cooled in the reactor pool and transported to facilities of JAERI for post-irradiation examination (PIE). Many kinds of data

<sup>\*</sup> Corresponding author: Tel.: +81-29 282 6939; fax: +81-29 282 6805; e-mail: nakano@jrr3fep2.tokai.jaeri.go.jp

Table 1  
Composition of ROX disks/mol%

Composition	Zirconia type	Thoria type
PuO <sub>2</sub>	10	10
Stabilized ZrO <sub>2</sub>	15	–
ThO <sub>2</sub>	–	15
Al <sub>2</sub> O <sub>3</sub>	65	65
MgO	10	10

<sup>a</sup> Composition of stabilized ZrO<sub>2</sub>: 88.8ZrO<sub>2</sub> + 11.0Y<sub>2</sub>O<sub>3</sub> + 0.2Gd<sub>2</sub>O<sub>3</sub> (mol%).

Table 2  
Isotopic abundance of plutonium used for the experiment

Isotope	Abundance (mol%)
Pu-238	< 0.01
Pu-239	94.33
Pu-240	5.27
Pu-241	0.40
Pu-242	< 0.01

have been obtained from PIEs. Burnup as fissions per initial (heavy) metal atom (FIMA), isotopic abundance of plutonium, minor actinides production rate to initial plutonium amount and production amount of FP nuclides were used as benchmark data to validate the calculations. The results of the PIEs are shown in Tables 3–5 with the calculated values.

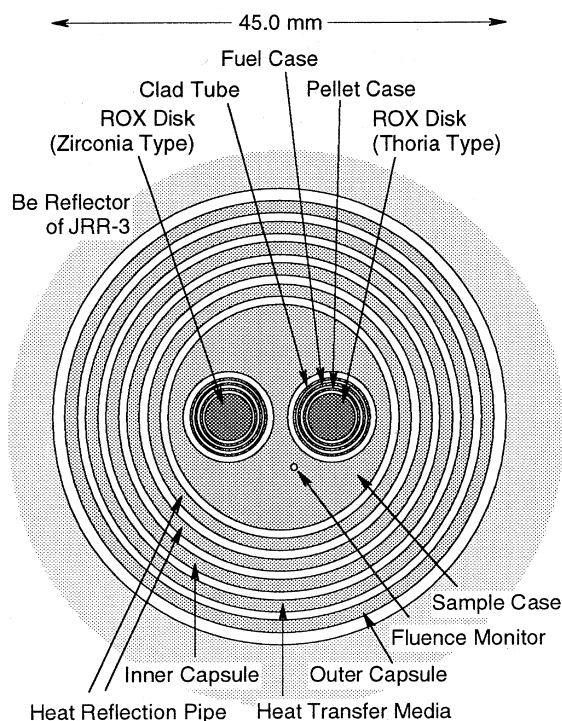


Fig. 1. Horizontal cross-section of the irradiation capsule.

Table 3  
Burnup of ROX disks/FIMA%

ROX disk	Measurement	SRAC (Cal./Meas.)	MVP-BURN (Cal./Meas.)
Zirconia type	27.90 0.087	29.82 (1.069)	31.51 (1.129)
Thoria type	27.95 0.137	30.68 (1.098)	32.07 (1.147)

The FP nuclides were evaluated by gamma ray measurement. Neodymium, uranium and plutonium were separated by an anion-exchange method. These elements were analyzed by mass-spectrometry using isotope dilution and hence their isotopic abundance was obtained. The number of fissions was evaluated from the amount of <sup>148</sup>Nd and its yield data for the <sup>239</sup>Pu thermal fission. The initial amount of plutonium was calculated as the sum of the number of fissions and the residual amount of plutonium. The FIMA burnup was determined by dividing the number of fissions by the initial amount of plutonium. During the error evaluation of the data, the error of the <sup>148</sup>Nd yield data was not included. It was difficult to evaluate it, because the fission reaction in a sample is mainly, but not only, due to the thermal fission of <sup>239</sup>Pu. After chemical separation, minor actinides were evaluated by alpha ray measurement.

The neutron capture rate of <sup>59</sup>Co was evaluated from the measurement of the gamma rays of cobalt used as a fluence monitor. This was used to normalize the power levels in the burnup calculations with the SRAC and the MVP-BURN codes.

## 4. Calculations

### 4.1. Computer codes and libraries

The SRAC [2] code system and the MVP-BURN [3] code were used for the calculations. Both of these codes have been developed by JAERI. SRAC is an integrated code system which consists of neutron cross-section libraries, a cell calculation module with burnup capability based on the collision probability method, core calculation modules based on Sn transport or diffusion theory and an auxiliary code for core burnup calculations. MVP-BURN is based on MVP [4], a continuous energy Monte Carlo code, which was completed with a burnup capability. The cross-section libraries for these computer codes are based on JENDL-3.2 [5].

### 4.2. Calculation of source spectrum

As a first step of the calculations, the neutron spectrum in the irradiation hole was calculated by SRAC. Using PIJ, a cell calculation module based on the

Table 4  
Microscopic absorption rate of Pu-239

ROX Disk	Code	Cycle-1	Cycle-2	Cycle-3	Cycle-4
Zirconia type	SRAC	$5.967 \times 10^{16}$	$6.437 \times 10^{16}$	$6.671 \times 10^{16}$	$6.845 \times 10^{16}$
	MVP-BURN	$6.125 \times 10^{16}$	$6.832 \times 10^{16}$	$7.350 \times 10^{16}$	$6.906 \times 10^{16}$
	1 $\sigma$ error	1.376%	1.360%	1.411%	1.545%
Thoria type	SRAC	$6.406 \times 10^{16}$	$6.601 \times 10^{16}$	$6.830 \times 10^{16}$	$6.998 \times 10^{16}$
	MVP-BURN	$6.584 \times 10^{16}$	$7.026 \times 10^{16}$	$7.113 \times 10^{16}$	$6.892 \times 10^{16}$
	1 $\sigma$ error	1.435%	1.419%	1.412%	1.396%

Table 5  
Microscopic fission rate of Pu-239

ROX disk	Code	Cycle-1	Cycle-2	Cycle-3	Cycle-4
Zirconia type	SRAC	$4.079 \times 10^{16}$	$4.406 \times 10^{16}$	$4.564 \times 10^{16}$	$4.678 \times 10^{16}$
	MVP-BURN	$4.263 \times 10^{16}$	$4.769 \times 10^{16}$	$5.125 \times 10^{16}$	$4.797 \times 10^{16}$
	1 $\sigma$ error	1.794%	1.777%	1.837%	2.014%
Thoria type	SRAC	$4.388 \times 10^{16}$	$4.518 \times 10^{16}$	$4.671 \times 10^{16}$	$4.780 \times 10^{16}$
	MVP-BURN	$4.580 \times 10^{16}$	$4.892 \times 10^{16}$	$4.941 \times 10^{16}$	$4.807 \times 10^{16}$
	1 $\sigma$ error	1.875%	1.843%	1.842%	1.824%

collision probability method, effective homogenized cross-sections of the fuel elements of the reactor were generated for 72 energy groups. After cell calculation, a diffusion whole core calculation in 2 dimensions and 72 energy groups was carried out using the cross-sections. CITATION included in the SRAC system was used for the calculation. From this calculation, the energy spectrum in the irradiation hole was obtained in 72 neutron groups. This spectrum was used as the fixed boundary source for the burnup calculations with the SRAC and the MVP-BURN codes.

#### 4.3. SRAC-BURNUP calculation

For the burnup calculation with SRAC, the PIJ module was used. Fig. 2 shows the calculational model. Not only ROX disks and capsule structures are included but a cobalt fluence monitor is also taken into account in the model. The vertical direction was treated as infinite. Narrow gaps between capsule structures, which could be seen in Fig. 1 were smeared. The fuel case of platinum was neglected because there were no cross-sections for platinum in the SRAC library. Using this model, a fixed source problem was solved in 72 energy groups. The neutron spectrum already obtained was used as the outer boundary neutron source into the capsule. Fine group flux distribution and effective cross-section of the ROX disks were obtained from the calculation and they were collapsed into one energy group. A nuclide depletion calculation was performed using the one group cross-section and the flux. The power level used in the calculation was normalized so as to give the same

reaction rate in the fluence monitor as that was the case in the experiment. Nuclide densities of the disks were calculated by this method and used for the next step, the fixed source calculation. Repeating these steps, results of burnup calculations were obtained.

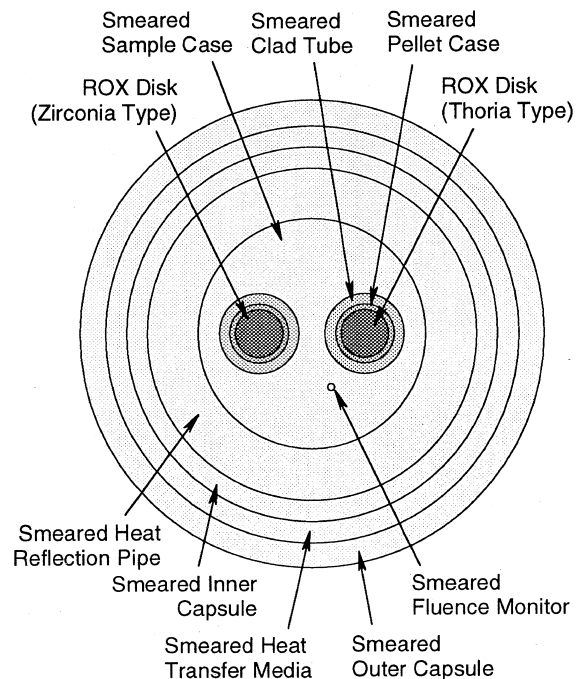


Fig. 2. SRAC calculational model.

#### 4.4. MVP-BURN calculation

As the MVP-BURN is a Monte Carlo code, it can handle complicated geometries with a minimum of approximations. The methodology of burnup calculations for MVP-BURN is the same as for SRAC. The MVP part of the code calculates reaction rates of nuclides and the BURN part of the code calculates depletion and nuclide densities for the next MVP step. Unfortunately, as the BURN part cannot handle the errors of the reaction rates coming from the MVP part, the errors of the final densities of the nuclides are not available.

MVP-BURN calculations have been performed with a three-dimensional model that represents the effective part of the capsule structure as exactly as possible. The horizontal model used in the calculations is the same as shown in Fig. 1 except that the platinum tube is neglected because there were no cross-sections for platinum in the MVP-BURN library. The vertical cross-section of the three-dimensional model is shown in Fig. 3.

#### 5. Calculated results and discussions

The results of burnup are shown in Table 3. The burnup values calculated with SRAC are slightly higher than the experimental values but differences are not very big for either the zirconia or the thoria type ROX disks. The MVP-BURN code overestimates the measured values by 13–15% in both cases. To investigate the difference between the two codes, the microscopic reaction rates of  $^{239}\text{Pu}$  were checked. Tables 4 and 5 show  $^{239}\text{Pu}$  microscopic reaction rates calculated by the two codes at the beginning of each burnup cycle. For all cycles, reaction rates of MVP-BURN are larger than those of SRAC, except for the case of the thoria type in cycle 4. Fig. 4 shows neutron spectra of ROX disks. It can be seen that the spectrum in the thoria disk is softer than that in the zirconia disk, because the amount of plutonium in a thoria disk is slightly smaller than that of a zirconia disk. Therefore, for  $^{239}\text{Pu}$ , the one group microscopic absorption cross-sections and reaction rates of the thoria disk become larger than that of the zirconia disk. The spectra calculated by MVP-BURN are softer than those given by SRAC, because in the SRAC model, neutron leakage on the vertical direction is considered by a buckling value, which is applied for all energy groups. The real structure of the irradiation capsule has several vertical void gaps and fast neutrons can easily escape from the capsule. In the MVP-BURN model, vertical void gaps are included as exactly as possible and energy-dependent neutron leakage is included in the results. It makes the MVP-BURN spectra softer than the SRAC ones.

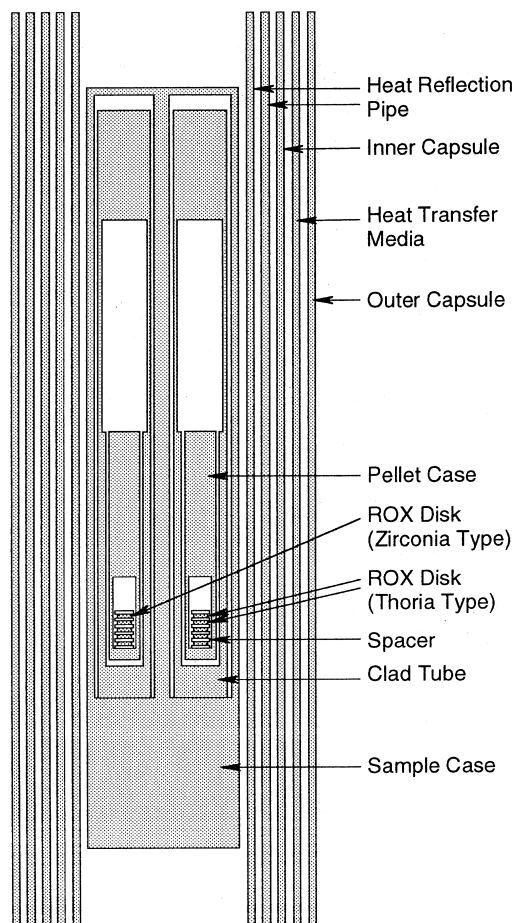


Fig. 3. Vertical cross-section of MVP-BURN calculational model.

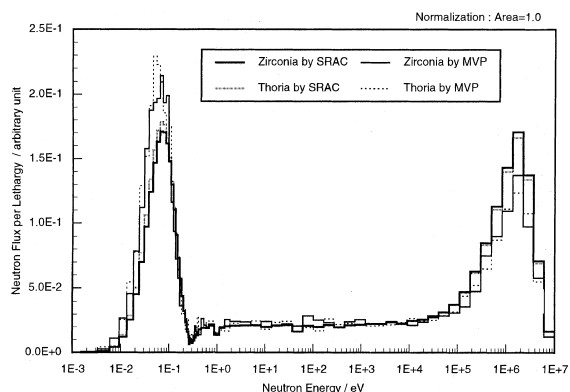


Fig. 4. Neutron spectra of ROX disks before irradiation.

The isotopic abundance results of plutonium are shown in Table 6. The calculated results agree moderately well with the measured values. The calculated  $^{239}\text{Pu}$

Table 6  
Isotopic abundance of plutonium after irradiation (at.%)

ROX disk	Isotope	Measurement	SRAC	MVP-BURN
Zirconia type	Pu-238	0.020	0.01	0.01
		0.0002		
	Pu-239	75.491	74.65	74.18
		0.0025		
	Pu-240	20.073	22.16	22.52
		0.0032		
	Pu-241	4.046	2.89	2.97
0.0008				
Pu-242	0.370	0.30	0.32	
	0.0004			
Final Pu to initial Pu	72.10	70.69	69.08	
	0.087			
Thoria type	Pu-238	0.022	0.01	0.01
		0.0006		
	Pu-239	75.494	73.96	73.95
		0.0015		
	Pu-240	19.818	22.69	22.31
		0.0017		
	Pu-241	4.281	3.02	3.34
0.0007				
Pu-242	0.385	0.32	0.39	
	0.0007			
Final Pu to initial Pu	72.05	69.90	68.59	
	0.137			

abundance values are smaller than the measured ones. This is consistent with the overestimation of the calculated burnup compared to the measurements.

Production ratios of americium and curium to initial plutonium atoms are listed in Table 7. All calculations

largely underestimate the measured values. A large discrepancy cannot be seen between the two codes, because the burnup chain for minor actinides, the depletion calculation methodology and the base neutron cross-section libraries are the same for both codes. As the

Table 7  
Production ratio of Am, Cm and U atoms relative to the initial number of Pu atoms

ROX disk	Isotope	Measurement <sup>a</sup>	SRAC (Cal./Meas.)	MVP-BURN (Cal./Meas.)
Zirconia type	Am-241	$3.046 \times 10^{-3}$	$2.142 \times 10^{-3}$	$2.132 \times 10^{-3}$
		0.16%	(0.703)	(0.700)
	Cm-242	$2.985 \times 10^{-6}$	$1.901 \times 10^{-6}$	$1.928 \times 10^{-6}$
		0.16%	(0.637)	(0.646)
Cm-244	$3.988 \times 10^{-6}$	$1.065 \times 10^{-6}$	$1.111 \times 10^{-6}$	
	0.80%	(0.267)	(0.279)	
Thoria type	Am-241	$3.226 \times 10^{-3}$	$2.213 \times 10^{-3}$	$2.397 \times 10^{-3}$
		0.16%	(0.686)	(0.743)
	Cm-242	$3.124 \times 10^{-6}$	$1.996 \times 10^{-6}$	$2.226 \times 10^{-6}$
		0.14%	(0.639)	(0.713)
	Cm-244	$4.839 \times 10^{-6}$	$1.157 \times 10^{-6}$	$1.548 \times 10^{-6}$
		0.66%	(0.239)	(0.320)
	U-233 <sup>a</sup>	$5.450 \times 10^{-3}$	$7.182 \times 10^{-3}$	$7.608 \times 10^{-3}$
0.55%		(1.318)	(1.396)	

<sup>a</sup> Other U isotopes: less than detection limit.

calculated FIMA burnups are not very different from the measured values, the present calculation method seems adequate. Therefore, the discrepancy may not be only due to the calculation method. To see the effect of  $^{240}\text{Pu}$  and  $^{241}\text{Pu}$  cross-sections, two MVP-BURN calculations were done using cross-sections based on ENDF/B-VI [6] only for  $^{240}\text{Pu}$  or  $^{241}\text{Pu}$ . The reason for this choice is that  $^{241}\text{Am}$  is mainly produced by n-gamma reactions of  $^{240}\text{Pu}$  and beta decays of  $^{241}\text{Pu}$ .

Table 8 shows the isotopic abundance of plutonium and Table 9 shows the production ratios of americium and curium using ENDF/B-VI cross-sections for  $^{240}\text{Pu}$  or  $^{241}\text{Pu}$  and JENDL-3.2 cross-sections for the other nuclides. When the  $^{240}\text{Pu}$  cross-sections are changed from JENDL-3.2 to ENDF/B-VI, the  $^{240}\text{Pu}$  abundance of the zirconia disk becomes smaller and the  $^{241}\text{Pu}$  abundance becomes larger. Therefore, the production ratios of  $^{241}\text{Am}$  and  $^{242}\text{Cm}$  become larger. In contrast with this, the  $^{240}\text{Pu}$  abundance of the thoria disk

becomes larger and the  $^{241}\text{Pu}$  abundance becomes smaller. Therefore, the production ratios of  $^{241}\text{Am}$  and  $^{242}\text{Cm}$  become smaller. Table 10 shows the  $^{240}\text{Pu}$  capture rate of each library. In the case of the zirconia disk, the  $^{240}\text{Pu}$  reaction rate of ENDF/B-VI is larger than that of JENDL-3.2. It makes the  $^{240}\text{Pu}$  abundance of ENDF/B-VI smaller than that of JENDL-3.2. The reverse can be observed in the thoria disk case.

When  $^{241}\text{Pu}$  cross-sections are changed from JENDL-3.2 to ENDF/B-VI, the effect is smaller than for changing  $^{240}\text{Pu}$  cross-sections. Table 11 shows  $^{241}\text{Pu}$  capture rates of each library. In case of the zirconia disk,  $^{241}\text{Pu}$  capture rates from ENDF/B-VI are larger than those from JENDL-3.2 at cycles 1 and 4. At cycle 2 only, ENDF/B-VI reaction rates are smaller than those from JENDL-3.2. Therefore,  $^{241}\text{Pu}$  abundance and production ratios of the three actinide isotopes become larger with ENDF/B-VI. In the case of the thoria disk, there is no systematic difference in the  $^{241}\text{Pu}$  capture rates between both

Table 8  
Isotopic abundance of plutonium after irradiation using ENDF/B-VI cross-sections for Pu-240 and Pu-241/atom%

ROX disk	Isotope	MVP-BURN JENDL-3.2 only	MVP-BURN ENDF/B-VI for Pu-240	MVP-BURN ENDF/B-VI for Pu-241
Zirconia type	Pu-238	0.01	0.01	0.01
	Pu-239	74.18	74.15	74.20
	Pu-240	22.52	22.28	22.34
	Pu-241	2.97	3.21	3.11
	Pu-242	0.32	0.36	0.34
Thoria type	Pu-238	0.01	0.01	0.01
	Pu-239	73.95	73.95	74.06
	Pu-240	22.31	22.66	22.20
	Pu-241	3.34	3.05	3.36
	Pu-242	0.39	0.34	0.38

Table 9  
Production ratio of Am and Cm atoms relative to the initial number of Pu atoms using ENDF/B-VI cross-sections for Pu-240 and Pu-241

ROX disk	Isotope	MVP-BURN JENDL-3.2 only (Cal./Meas.)	MVP-BURN ENDF/B-VI for Pu-240 (Cal./Meas.)	MVP-BURN ENDF/B-VI for Pu-241 (Cal./Meas.)
Zirconia type	Am-241	$2.132 \times 10^{-3}$ (0.700)	$2.309 \times 10^{-3}$ (0.758)	$2.235 \times 10^{-3}$ (0.734)
	Cm-242	$1.928 \times 10^{-6}$ (0.646)	$2.127 \times 10^{-6}$ (0.712)	$2.091 \times 10^{-6}$ (0.701)
	Cm-244	$1.111 \times 10^{-6}$ (0.279)	$1.112 \times 10^{-6}$ (0.279)	$1.505 \times 10^{-6}$ (0.377)
Thoria type	Am-241	$2.397 \times 10^{-3}$ (0.743)	$2.180 \times 10^{-3}$ (0.676)	$2.409 \times 10^{-3}$ (0.747)
	Cm-242	$2.226 \times 10^{-6}$ (0.713)	$2.016 \times 10^{-6}$ (0.645)	$2.239 \times 10^{-6}$ (0.717)
	Cm-244	$1.548 \times 10^{-6}$ (0.320)	$1.689 \times 10^{-6}$ (0.349)	$1.545 \times 10^{-6}$ (0.319)

Table 10  
Pu-240 microscopic capture rate at each burnup cycle calculated by MVP

ROX Disk	Library	Cycle-1	Cycle-2	Cycle-3	Cycle-4
Zirconia type	JENDL-3.2	$2.674 \times 10^{16}$	$2.799 \times 10^{16}$	$2.670 \times 10^{16}$	$2.877 \times 10^{16}$
	1 $\sigma$ error	7.485%	6.481%	5.409%	7.229%
	ENDF/B-VI	$3.274 \times 10^{16}$	$3.158 \times 10^{16}$	$3.262 \times 10^{16}$	$2.753 \times 10^{16}$
	1 $\sigma$ error	9.177%	8.680%	8.420%	6.102%
Thoria type	JENDL-3.2	$3.432 \times 10^{16}$	$3.498 \times 10^{16}$	$3.366 \times 10^{16}$	$2.808 \times 10^{16}$
	1 $\sigma$ error	11.416%	8.744%	10.173%	6.409%
	ENDF/B-VI	$2.872 \times 10^{16}$	$2.817 \times 10^{16}$	$3.062 \times 10^{16}$	$2.733 \times 10^{16}$
	1 $\sigma$ error	7.368%	6.270%	6.918%	6.575%

Table 11  
Pu-241 microscopic capture reaction rate at each burnup cycle calculated by MVP

ROX disk	Library	Cycle-1	Cycle-2	Cycle-3	Cycle-4
Zirconia type	JENDL-3.2	$1.859 \times 10^{16}$	$2.086 \times 10^{16}$	$2.229 \times 10^{16}$	$2.066 \times 10^{16}$
	1 $\sigma$ error	1.832%	1.866%	1.888%	2.064%
	ENDF/B-VI	$1.865 \times 10^{16}$	$2.075 \times 10^{16}$	$2.229 \times 10^{16}$	$2.110 \times 10^{16}$
	1 $\sigma$ error	1.947%	1.925%	1.940%	1.944%
Thoria type	JENDL-3.2	$2.005 \times 10^{16}$	$2.129 \times 10^{16}$	$2.148 \times 10^{16}$	$2.105 \times 10^{16}$
	1 $\sigma$ error	1.968%	1.884%	1.905%	1.893%
	ENDF/B-VI	$1.998 \times 10^{16}$	$2.134 \times 10^{16}$	$2.157 \times 10^{16}$	$2.037 \times 10^{16}$
	1 $\sigma$ error	1.924%	1.918%	1.983%	1.913%

libraries. Therefore, the  $^{241}\text{Pu}$  abundance and production ratios of the three actinide isotopes do not change.

## 6. Conclusions

An irradiation experiment concerning two kinds of ROX disks and their burnup analysis was performed. The results of burnup calculations were compared with the measured values obtained from the post-irradiation examinations. The calculations of burnup overestimate the measured values. The MVP-BURN code gives higher burnup values than the SRAC code, because the MVP-BURN calculations include the fast neutron leakage on the vertical direction.

The calculated plutonium isotopic abundance shows a fair agreement with the measured value. No large differences can be observed between the two codes.

Production ratios of americium and curium calculated by both codes are much smaller than the measured values. Changing  $^{240}\text{Pu}$  or  $^{241}\text{Pu}$  cross-sections from JENDL-3.2 to ENDF/B-VI does not affect the results very much. Therefore, these cross-sections are not the major reason for the observed discrepancies. The large differences in small quantities of americium and curium isotope contents stem from the rather low initial abundance of the higher plutonium isotopes.

## Acknowledgements

The authors wish to present their great thanks to the staff who involved ROX disk fabrication, irradiation experiment and post-irradiation examinations. They would also like to express their appreciation to Mr K. Okumura, Mr Y. Nagaya, Dr T. Mori and Mr K. Kaneko for their help in using the computer codes.

## References

- [1] H. Takano, H. Akie, T. Muromura, Proc. Sixth International Conference on Nuclear Engineering. (ICONE-6), San Diego, CA, USA, 10–14 May 1998, ASME, 1998.
- [2] K. Okumura, K. Kunio, K. Tsuchihashi, SRAC95; General purpose neutronics code system, Japan Atomic Energy Research Institute Report JAERI-Data/Code 96-015, 1996 (in Japanese).
- [3] K. Okumura, M. Nakagawa, K. Kaneko, Proc. Joint International Conference on Mathematical Methods and Supercomputing for Nuclear Applications, Saratoga Springs, New York, USA, 5–9 October 1997, ANS, 1997.
- [4] T. Mori, M. Nakagawa, MVP/GMVP: General purpose monte carlo codes for neutron and photon transport calculations based on continuous energy and multigroup methods, Japan Atomic Energy Research Institute Report JAERI-Data/Code 94-007, 1994 (in Japanese).

- [5] T. Nakagawa, K. Shibata, S. Chiba, T. Fukahori, Y. Nakajima, Y. Kikuchi, T. Kawano, Y. Kanda, T. Ohsawa, H. Matsunobu, M. Kawai, A. Zukeran, T. Watanabe, S. Igarasi, K. Kosako, T. Asami, *J. Nucl. Sci. Technol.* 32 (1995) 1259.
- [6] P.F. Rose (Comp. and Ed.), ENDF-201, ENDF/B-VI Summary documentation, Brookhaven National Laboratory Report BNL-NCS-17541, 4th ed., 1991.